ЯДЕРНА ФІЗИКА
NUCLEAR PHYSICS

УДК 539.142 https://doi.org/10.15407/jnpae2023.04.336

K. A. Gado[1,2,*]

[1] *Department of Physics, Faculty of Science and Arts, Al-Mikhwah, Al-Baha University, Al-Baha, Saudi Arabia*
[2] *Basic Sciences Department, Bilbeis Higher Institute for Engineering, Bilbeis, Sharqia, Egypt*

*Corresponding author: qjado76@gmail.com

IMPORTATION OF BAND HEAD SPIN FOR SUPERDEFORMED BANDS IN MASS REGION A ~ 60 - 90 USING THE VARIABLE MOMENT OF INERTIA MODEL

We are currently applying the variable moment of inertia model to nuclei in mass region A ~ 60 - 90 in order to improve spectroscopic analysis of its rotational bands in the superdeformed region, which in turn is helpful in the band head spin prediction and other spins for superdeformed bands. The moment of inertia of the ground state, ϑ_0 and restoring force constant, *C*, were calculated by fitting the observed transition energies. The band head spin, I_0 was determined in terms of the ratio of transition energies, verified by root mean square deviations. We verified that the observed high spin superdeformed bands display a near-rigid rotor behavior by studying transition energies over twice the angular momentum (RTEOS). The calculated and observed transition energies agree well.

Keywords: superdeformed band, spin assignment, variable moment of inertia model.

1. Introduction

Since the discovery of the first superdeformed (SD) band in ^{152}Dy, the subject of superdeformation has been at the forefront of nuclear structure physics [1, 2]. There are currently experimental data on SD rotational bands in the $A \cong 80, 130, 150,$ and 190 mass regions, respectively, of the periodic table [3 - 6]. The SD mass region $A \cong 60-90$ is of particular interest because of the limited number of particles found in these nuclei and the fact that they have the lightest masses and, consequently, the highest rotational frequencies [7]. Furthermore, these SD nuclei have received poor theoretical research. Most of the SD bands in this mass range behave similarly in terms of their dynamic moment of inertia and rotational frequency i.e., they exhibit a smooth decrease as frequency increases. Gamma-ray energies are sadly the only generally accessible spectroscopic data for the SD bands. Due to the discrete connecting transitions between the low-lying states during normal deformation (ND) and the SD states not being observed. Poor experimental data exist for the spin of the rotational bands, making theoretical calculations the sole option to determine the spin value. Spins have been assigned to SD states using a variety of methods. These strategies use both direct and indirect techniques to give the states in SD bands a spin [8 - 10]. The specifics of the variable moment of inertia (VMI) model are covered in Section II of this study, which is organized as follows. Section III contains the results and commentary. The work's conclusions are presented at the end.

2. Mathematical model

Mariscotti et al. [11, 12] were the ones who initially suggested the VMI model in order to forecast the various level energies of ground state bands in even-even nuclei. This approach effectively generalizes the ratio of the greater mass nucleus and represents the rotational energy as an expansion in terms of $I(I+1)$. The sum of the potential energy term and the rotational energy term yields the VMI equation for rotational bands:

$$E_I = E_0 + \frac{\left[I(I+1) - I_0(I_0+1)\right]}{2\vartheta_I} + \frac{C(\vartheta_I - \vartheta_0)^2}{2}. \quad (1)$$

The first term indicates the band head's energy, E_0. Rotational energy is represented by the second term, where I is angular momentum, I_0 the band head's angular momentum and ϑ_I is the corresponding moment of inertia of the state with angular momentum I. The potential energy is the third term, where C is restoring force constant (stiffness parameter), ϑ_0 the band head's moment of inertia.

Utilizing the equilibrium condition

$$\frac{\partial E(\vartheta_I)}{\partial \vartheta_I} = 0, \quad (2)$$

we are able to rewrite Eq. (1) as:

$$-\frac{\left[I(I+1) - I_0(I_0+1)\right]}{2\vartheta_I^2} + C(\vartheta_I - \vartheta_0) = 0. \quad (3)$$

Also, we rewrite this equation as

$$\vartheta_I^3 - \vartheta_0\vartheta_I^2 - \frac{\left[I(I+1) - I_0(I_0+1)\right]}{2C} = 0. \quad (4)$$

This cubic equation has one real root for any positive value of ϑ_0 and C. Using Eq. (3), we may rewrite Eq. (1) as follows:

$$E_I = E_0 + \frac{\left[I(I+1) - I_0(I_0+1)\right]}{2\vartheta_I} + \frac{\left[I(I+1) - I_0(I_0+1)\right]^2}{8C\vartheta_I^4}. \quad (5)$$

In adiabatic limit, $\vartheta_I = \vartheta_0$. This leads to the following expression

$$E_I = E_0 + \frac{\left[I(I+1) - I_0(I_0+1)\right]}{2\vartheta_0} + \frac{\left[I(I+1) - I_0(I_0+1)\right]^2}{8C\vartheta_0^4}. \quad (6)$$

The transition energy for SD bands is written as:

$$E_\gamma(I \to I-2) = E(I) - E(I-2). \quad (7)$$

$$E_\gamma(I \to I-2) = \frac{\left[I(I+1) - (I-2)(I-1)\right]}{2\vartheta_0} + \frac{\left[I(I+1) - (I-2)(I-1)\right]^2}{8C\vartheta_0^4}. \quad (8)$$

For a SD band cascade we have

$$I_0 + 2n \to I_0 + 2n - 2 \to \ldots I_0 + 2 \to I_0, \quad (9)$$

The transition energies are: $E_\gamma(I_0+2n)$, $E_\gamma(I_0+2n-2)$, $E_\gamma(I_0+2n-4)$, …, $E_\gamma(I_0+4)$, $E_\gamma(I_0+2)$. Fitting with Eq. (8) the observed transition energies, the parameters ϑ_0 and C values are determined. The ratio of transition energies may be used to calculate the band head spin as:

$$R = \frac{E_\gamma(I+2 \to I)}{E_\gamma(I \to I-2)}. \quad (10)$$

The root mean square (rms) deviations of the transition energies computed at various I_0-values were used to confirm the accuracy of the band head spin:

$$\text{rms} = \left[\frac{1}{N}\sum_{i=1}^{N}\left|\frac{E_\gamma^{cal}(I_i) - E_\gamma^{exp}(I_i)}{E_\gamma^{exp}(I_i)}\right|^2\right]^{\frac{1}{2}}. \quad (11)$$

Here N is the total number of fitted transitions, and transition energies over twice spin (RTEOS).

3. Results and discussion

The band head spin of all the 13 known bands in ^{58}Ni (b_1), ^{58}Cu, ^{59}Cu (b_1), ^{61}Zn, ^{62}Zn, ^{65}Zn, ^{68}Zn, ^{84}Zr, ^{86}Zr (b_1), ^{88}Mo (b_1, b_2, b_3) and ^{89}Tc nuclei were determined in the form of the gamma transition energy ratio, Eq. (10). The comparison with other theoretical results is given in Table 1.

Table 1. **The band head spin I_0 for isotopes together with the computed transition energy, as well as the values from the available theoretical models and the stiffness constant (C) and band head moment of inertia (ϑ_0) utilized in the fitting**

SD band	$E_\gamma^{Exp}(I_0 \to I_0-2)$, MeV	$E_\gamma^{VMI}(I_0 \to I_0-2)$, MeV	C, MeV^3	ϑ_0, MeV^{-1}	I_0			
					Present assigned	Ref. [13]	Ref. [14]	Exp. [4]
^{58}Ni(b_1)	1.6630	1.6693	0.0625	20.68	13	13	17	15
^{58}Cu	0.8300	0.8969	0.0257	21.61	4	8	15	9
^{59}Cu(b_1)	1.5990	1.6121	0.0935	19.74	12.5	13.5	20.5	–
^{61}Zn	1.4320	1.3837	1.2700	17.52	13.5	17.5	23.5	12.5
^{62}Zn	1.9930	1.9773	1.1400	18.10	18	22	26	–
^{65}Zn	1.3410	1.2574	0.3010	19.68	20.5	12.5	21.5	–
^{68}Zn	1.5060	1.5106	0.3190	22.64	14	18	27	–
^{84}Zr	1.5260	1.5119	0.9770	27.40	21	25	36	–
^{86}Zr(b_1)	1.5180	1.4846	0.1080	32.40	28	27	37	–
^{88}Mo(b_1)	1.2380	–	0.0044	67.06	–	27	29	–
^{88}Mo(b_2)	1.4580	1.4585	0.0171	49.13	32	24	28	–
^{88}Mo(b_3)	1.2600	–	0.0054	65.76	–	23	30	–
^{89}Tc	1.1470	1.1189	0.2420	30.99	20.5	23.5	33.5	–

Table 1 presents two parameters, the band head moment of inertia ϑ_0 and the restoring constant, C, which are found by fitting empirically observed transition energies to the VMI model equation, Eq. (8). It is observed that calculated transition energies of studied nuclei compare well to observed transition energies, except ^{88}Mo (b_1) and ^{88}Mo (b_3), the reason for this is due to not calculating the band head spin, I_0, which depends on the discriminant of Eq. (10), and its value in both cases is not positive, b_1, b_2 and b_3 represent band1, band2 and band3, respectively. It is clear that the calculated band head spin is slightly less than the value quoted in the references [4, 13, 14] for ^{58}Ni(b_1) and ^{58}Cu except ^{61}Zn greater than only the experimental value. The calculated transition energies for different band head spin, I_0, with the rms deviations value of studied nuclei are given in Table 2.

Table 2. **The calculated transition energies for different band head spin (I_0) with the rms deviation value of studied nuclei**

Nucleus	^{58}Ni(b_1)					
Band head spin	I_0					
	12		13		14	
$E_\gamma^{Exp}(I \to I-2)$, MeV	I	$E_\gamma^{VMI}(I \to I-2)$, MeV	I	$E_\gamma^{VMI}(I \to I-2)$, MeV	I	$E_\gamma^{VMI}(I \to I-2)$, MeV
1.663	14	1.521	15	1.669	16	1.824
1.989	16	1.824	17	1.988	18	2.161
2.350	18	2.161	19	2.342	20	2.534
2.750	20	2.534	21	2.735	22	2.948
3.157	22	2.948	23	3.171	24	3.407
rms	0.078833124		0.003772264		0.083198058	
Nucleus	^{58}Cu					
Band head spin	3		4		5	
0.83	5	0.433	6	0.539	7	0.651
1.197	7	0.651	8	0.770	9	0.896
1.576	9	0.896	10	1.032	11	1.178
1.955	11	1.178	12	1.336	13	1.505
2.342	13	1.505	14	1.688	15	1.886
2.748	15	1.886	16	2.098	17	2.328
rms	0.409367931		0.316858842		0.218591322	
Nucleus	^{59}Cu(b_1)					
Band head spin	11.5		12.5		13.5	
1.599	13.5	1.472	14.5	1.612	15.5	1.757
1.900	15.5	1.757	16.5	1.910	17.5	2.068
2.242	17.5	2.068	18.5	2.234	19.5	2.408
2.611	19.5	2.408	20.5	2.590	21.5	2.780
3.004	21.5	2.780	22.5	2.979	23.5	3.187
3.424	23.5	3.187	24.5	3.405	25.5	3.633
3.827	25.5	3.633	26.5	3.872	27.5	4.122
rms	0.072401784		0.007613363		0.076481402	
Nucleus	^{61}Zn					
Band head spin	12.5		13.5		14.5	
1.432	14.5	1.620	15.5	1.739	16.5	1.859
1.626	16.5	1.859	17.5	1.980	18.5	2.102
1.845	18.5	2.102	19.5	2.225	20.5	2.348
2.082	20.5	2.348	21.5	2.473	22.5	2.599
2.307	22.5	2.599	23.5	2.725	24.5	2.853
2.545	24.5	2.853	25.5	2.982	26.5	3.113
2.818	26.5	3.113	27.5	3.244	28.5	3.377
3.127	28.5	3.377	29.5	3.512	30.5	3.647
3.466	30.5	3.647	31.5	3.785	32.5	3.924
rms	0.117757687		0.17661717		0.236192094	

Continuation of Table 2

Nucleus	^{62}Zn					
Band head spin	I_0					
	17		18		19	
$E_\gamma^{Exp}(I \to I-2)$, MeV	I	$E_\gamma^{VMI}(I \to I-2)$, MeV	I	$E_\gamma^{VMI}(I \to I-2)$, MeV	I	$E_\gamma^{VMI}(I \to I-2)$, MeV
1.993	19	2.095	20	2.215	21	2.335
2.215	21	2.335	22	2.456	23	2.579
2.440	23	2.579	24	2.702	25	2.827
2.690	25	2.827	26	2.953	27	3.080
2.939	27	3.080	28	3.208	29	3.338
3.236	29	3.338	30	3.469	31	3.602
rms	0.049655918		0.099280728		0.149497486	
Nucleus	^{65}Zn					
Band head spin	19.5		20.5		21.5	
1.341	21.5	2.338573	22.5	2.470881	23.5	2.606111
1.491	23.5	2.606111	24.5	2.744397	25.5	2.885872
1.668	25.5	2.885872	26.5	3.030668	27.5	3.178918
1.887	27.5	3.178918	28.5	3.330755	29.5	3.486312
2.121	29.5	3.486312	30.5	3.645723	31.5	3.809118
2.362	31.5	3.809118	32.5	3.976632	33.5	4.148398
2.963	33.5	4.148398	34.5	4.324548	35.5	4.505215
3.005	35.5	4.505215	36.5	4.690532	37.5	4.880631
3.349	37.5	4.880631	38.5	5.075647	39.5	5.27571
rms	0.625633264		0.70277537		0.781809147	
Nucleus	^{68}Zn					
Band head spin	13		14		15	
1.506	15	1.316	16	1.413	17	1.510
1.717	17	1.510	18	1.609	19	1.709
1.918	19	1.709	20	1.810	21	1.913
2.121	21	1.913	22	2.017	23	2.122
2.331	23	2.122	24	2.229	25	2.338
2.555	25	2.338	26	2.449	27	2.561
2.795	27	2.561	28	2.676	29	2.792
3.037	29	2.792	30	2.910	31	3.031
rms	0.100164738		0.050491593		0.002744648	
Nucleus	^{84}Zr					
Band head spin	20		21		22	
1.526	22	1.587	23	1.663	24	1.738
1.663	24	1.738	25	1.815	26	1.891
1.808	26	1.891	27	1.968	28	2.045
1.959	28	2.045	29	2.122	30	2.199
2.114	30	2.199	31	2.277	32	2.356
2.272	32	2.356	33	2.434	34	2.513
2.435	34	2.513	35	2.592	36	2.672
2.599	36	2.672	37	2.752	38	2.832
2.761	38	2.832	39	2.913	40	2.995
rms	0.038429433		0.076795189		0.115392387	
Nucleus	^{86}Zr(b_1)					
Band head spin	27		28		29	
1.518	29	1.954	30	2.037	31	2.122
1.646	31	2.122	32	2.208	33	2.295
1.785	33	2.295	34	2.384	35	2.475
1.929	35	2.475	36	2.568	37	2.663
2.077	37	2.663	38	2.759	39	2.857
2.228	39	2.857	40	2.957	41	3.059
2.540	41	3.059	42	3.164	43	3.270
2.696	43	3.270	44	3.378	45	3.489
rms	0.267906567		0.315246781		0.363523283	

Continuation of Table 2

Nucleus	^{88}Mo(b_2)					
Band head spin	I_0					
	31		32		33	
$E_\gamma^{Exp}(I \to I-2)$, MeV	I	$E_\gamma^{VMI}(I \to I-2)$, MeV	I	$E_\gamma^{VMI}(I \to I-2)$, MeV	I	$E_\gamma^{VMI}(I \to I-2)$, MeV
1.458	33	1.668	34	1.741	35	1.817
1.596	35	1.817	36	1.894	37	1.974
1.743	37	1.974	38	2.056	39	2.14
1.895	39	2.14	40	2.226	41	2.315
2.051	41	2.315	42	2.407	43	2.500
2.229	43	2.500	44	2.597	45	2.696
rms	0.132571387		0.179204138		0.22711699	
Nucleus	^{89}Tc					
Band head spin	19.5		20.5		21.5	
1.147	21.5	1.397	22.5	1.467	23.5	1.539
1.259	23.5	1.539	24.5	1.611	25.5	1.683
1.384	25.5	1.683	26.5	1.756	27.5	1.830
1.521	27.5	1.830	28.5	1.905	29.5	1.980
1.668	29.5	1.980	30.5	2.057	31.5	2.134
1.818	31.5	2.134	32.5	2.212	33.5	2.290
1.975	33.5	2.290	34.5	2.370	35.5	2.450
2.136	35.5	2.450	36.5	2.532	37.5	2.614
2.298	37.5	2.614	38.5	2.698	39.5	2.782
2.459	39.5	2.782	40.5	2.868	41.5	2.954
2.625	41.5	2.954	42.5	3.042	43.5	3.131
rms	0.178146189		0.223751583		0.269844365	

Knowing that VMI and rms results differ by ± 1 value, it is obvious that the band head spin, I_0, given by the VMI equation for ^{61}Zn, ^{62}Zn, ^{65}Zn, ^{84}Zr, ^{86}Zr(b_1), ^{88}Mo(b_2), and ^{89}Tc is one greater than the minimum rms value, and the band head spin given by the VMI equation for ^{58}Ni(b_1) and ^{59}Cu(b_1) are in agreement with the minimum rms, similarly for ^{58}Cu and ^{68}Zn, the band head spin, I_0, given by the VMI equation is one less than the minimum rms value. In most cases, the computed values are in good agreement with the experimental data, meaning that the estimated energy spectra are accurately replicated. The spin value derived through rms deviation serves as proof of this computation.

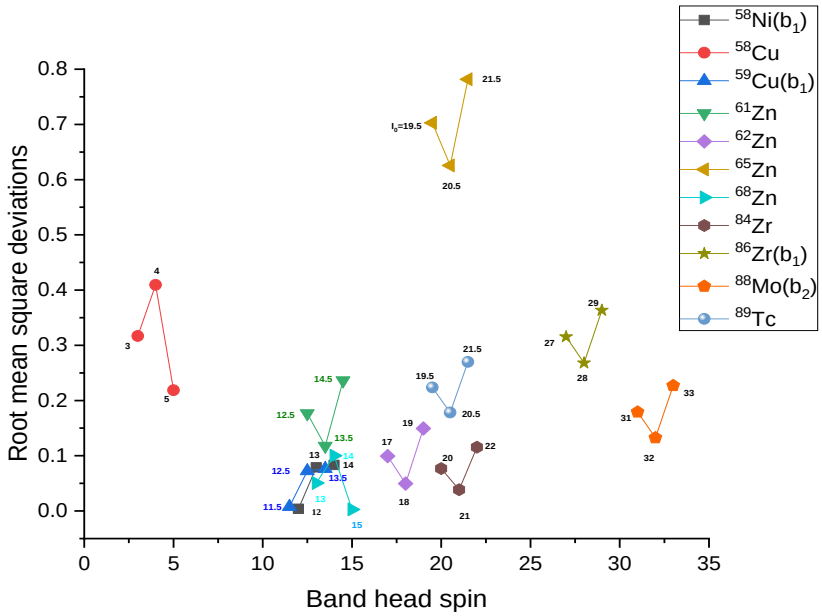

Fig. 1. The rms deviations as a function of band head spin (I_0) of studied nuclei.
(See color Figure on the journal website.)

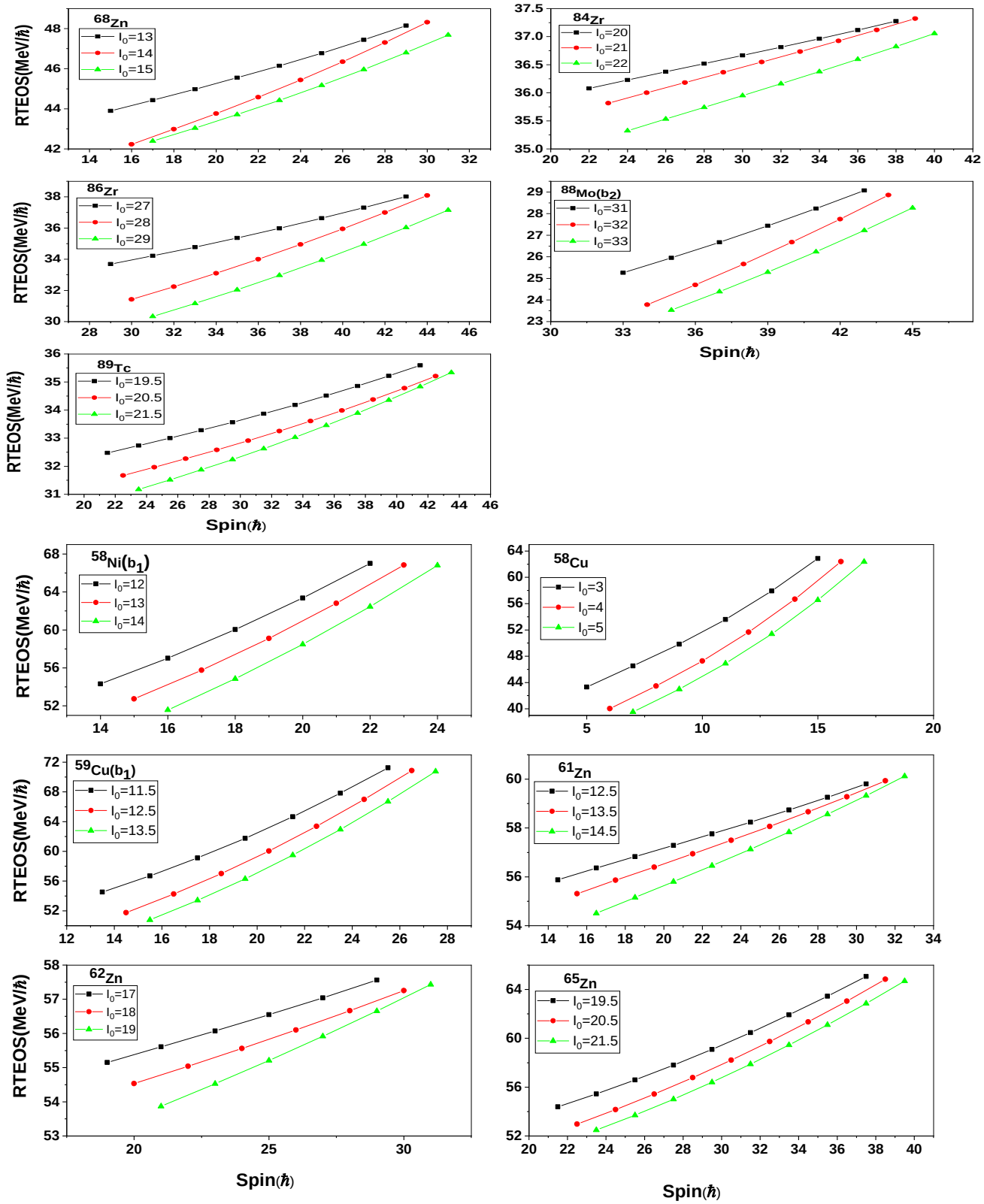

Fig. 2. The ratio of transition energies over twice spin (TEOS) as a function of spin (I) for studied nuclei. (See color Figure on the journal website.)

Fig. 1 presents the bands of nuclei ^{58}Ni(b_1), ^{59}Cu(b_1), ^{61}Zn and ^{68}Zn which are similar in terms of the band head spin, I_0, values and the range of rms deviations are greater than zero and less than 0.3, while the bands of nuclei ^{62}Zn, ^{65}Zn, ^{84}Zr, and ^{89}Tc are similar in terms of I_0, values, and the range of rms is greater than zero and less than 0.8, indicating that the values of the transition energies are similar. This is consistent with the idea that there are identical bands in the nuclei with masses between $A \cong 60$ and

$A \cong 90$. When examining the properties of the current nuclei, the quantity $\sigma = \frac{1}{2C\vartheta_0^3}$, is very helpful because it measures how soft the nucleus is. The nuclear softness parameter is connected to the rigidity of the nucleus and the rigidity of the nucleus increases with increasing superdeformation indicating near-rigid rotor behavior. Nuclear softness parameters for SD bands are in the range of $10^{-6} \le \sigma \le 10^{-4}$ [15]. When compared to the range of the study SD bands, which is $10^{-5} \le \sigma \le 10^{-3}$, it is obvious that the study SD bands are bigger than it and less than ND, $10^{-4} \le \sigma \le 10^{-2}$ [16, 17], which indicates that studied SD bands are significantly more rigid. This can be indicated by plotting the ratio of transition energies over twice spin (RTEOS) versus spin (I) shown in Fig. 2. If the band head spin, I_0, is set correctly, i.e., with high accuracy, so, the behavior of the curve resulting from drawing the relationship between the angular momentum and the ratio of the transition energies over twice the angular momentum is an approximation of a straight line (fixed) for the rigid rotating nuclei. But if the band head spin, I_0, deviates by ± 1 from the set value, the behavior of the curve is hyperbolic to the outside. Also, the deformation of these nuclei also increases, which indicates their semi-rigid behavior.

4. Conclusion

The VMI model is used to forecast the band-head spin (I_0) of 13 SD rotating bands in the $A \cong 60-90$ mass region. The rotational SD bands showed remarkably excellent rotational properties and rigid behavior. The recommended band-head spins had an impact on the transition energies. If the band-head spin value is accurately assigned, the rigid behavior has been validated by the relationship between ratio transition energies over twice spin $E_\gamma / 2I$ (RTEOS) and angular momentum (I). The estimated and observed transition energies are in good agreement. This method gives a very comprehensive interpretation of the spin assignment of SD rotational bands, which could help in designing future experiments for SD bands.

REFERENCES

1. P.J. Twin et al. Observation of a discrete-line superdeformed band up to 60ħ in ^{152}Dy. Phys. Rev. Lett. 57 (1986) 811.
2. M.A. Bentley et al. Intrinsic quadrupole moment of the superdeformed band in ^{152}Dy. Phys. Rev. Lett. 59 (1987) 2141.
3. A.V. Afanasjev, J. König, P. Ring. Superdeformed rotational bands in the A ~ 140 - 150 mass region: A cranked relativistic mean field description. Nucl. Phys. A 608 (1996) 107.
4. B. Singh, R.B. Firestone, S.Y.F. Chu. Table of superdeformed nuclear bands and fission isomers. Nucl. Data Sheets 78 (1996) 1.
5. C.E. Svensson et al. Decay out of the doubly magic superdeformed band in the N = Z nucleus ^{60}Zn. Phys. Rev. Lett. 82 (1999) 3400.
6. Z.X. Hu, J.Y. Zeng. Comparison of the Harris and ab expression for the description of nuclear superdeformed rotational bands. Phys. Rev. C 56 (1997) 2523.
7. T. Bäck et al. Observation of superdeformed states in ^{88}Mo. Eur. Phys. J. A 6 (1999) 391.
8. F.S. Stephens. Spin alignment in superdeformed rotational bands. Nucl. Phys. A 520 (1990) c91.
9. J.A. Becker et al. Level spin and moments of inertia in superdeformed nuclei near A = 194. Nucl. Phys. A 520 (1990) c187.
10. C.S. Wu et al. Spin determination and calculation of nuclear superdeformed bands in A ~ 190 region. Phys. Rev. C 45 (1992) 261.
11. M.A.J. Mariscotti, G. Scharff-Goldhaber, B. Buck. Phenomenological Analysis of Ground-State Bands in Even-Even Nuclei. Phys. Rev. 178 (1969) 1864.
12. A. Goel, U.V.S. Nair, A. Yadav. Band head spin assignment of Tl isotopes of superdeformed rotational bands. Cent. Eur. J. Phys. 12(9) (2014) 693.
13. A.S. Shalaby. Simple model calculations of spin and quantized alignment for the A ~ 60 - 90 superdeformed mass region. Acta Phys. Hung. A 25 (2006) 117.
14. K.A. Gado. Investigation of Identical Superdeformed Bands in Mass Region A ~ 60 - 90 Using the Modified Simple Model. Under publication (2023).
15. N. Sharma et al. Empirical evidence for magic numbers of superdeformed shapes. Phys. Rev. C 87 (2013) 024322.
16. A.S. Shalaby. Theoretical spin assignment and study of the A ~ 100 - 140 superdeformed mass region by using ab formula. Int. J. Phys. Sci. 9 (2014) 154.
17. V.S. Uma et al. Predicting superdeformed rotational band-head spin in A ~ 190 mass region using variable moment of inertia model. Pramana J. Phys. 86 (2016) 185.

К. А. Гадо[1,2,*]

[1] Кафедра фізики, факультет природничих наук і мистецтв, Аль-Міхва, Університет Аль-Баха, Аль-Баха, Саудівська Аравія
[2] Кафедра фундаментальних наук, Більбейський Вищий інженерний інститут, Більбейс, Шаркія, Єгипет

*Відповідальний автор: qjado76@gmail.com

ВИЗНАЧЕННЯ СПІНУ ГОЛОВНОЇ СМУГИ ДЛЯ СУПЕРДЕФОРМОВАНИХ ЯДЕР З МАСАМИ A ~ 60 – 90 З ВИКОРИСТАННЯМ МОДЕЛІ ЗІ ЗМІННИМ МОМЕНТОМ ІНЕРЦІЇ

Ми застосовуємо модель змінного моменту інерції до ядер в області мас A ~ 60 – 90 для покращення спектроскопічного аналізу смуг обертання в супердеформованій області, що, в свою чергу, допомагає визначити спін головної смуги та інших супердеформованих смуг. Момент інерції основного стану $\Im_0$ і відновлювальна силова константа C були розраховані підгоною теоретичних енергій переходу до спостережуваних. Спін головної смуги I_0 був визначений за допомогою відношення енергій переходів за мінімумом середніх квадратичних відхилень. Отримані високі спіни супердеформованих смуг демонструють поведінку близьку до жорсткого ротора при вивченні залежності енергій переходу від подвійного кутового моменту (RTEOS). Розраховані та спостережувані енергії переходу добре узгоджуються.

Ключові слова: супердеформована смуга, визначення спіну, модель змінного моменту інерції.

Надійшла/Received 01.07.2023